remote sensing

MDPI

Article

Spatio-Temporal Evolution of Urban Expansion along Suburban Railway Lines in Megacities Based on Multi-Source Data: A Case Study of Beijing, China

Hongya Tang [1,2], Xin Yan [1], Tianshu Liu [1] and Jie Zheng [1,*]

[1] School of Textile Engineering and Art, Anhui Agricultural University, Hefei 230036, China; tanghongya@ahau.edu.cn (H.T.); yanxin0321@stu.ahau.edu.cn (X.Y.); liutianshu@stu.ahau.edu.cn (T.L.)
[2] School of Geography and Tourism, Anhui Normal University, Wuhu 241003, China
* Correspondence: zj_1229@njfu.edu.cn

Abstract: Suburban railways in megacities exert a pivotal role in propelling urbanization and shaping urban agglomeration. However, previous study endeavors have overlooked the transformations occurring in urban expansion along suburban railways, with a particular dearth of attention on the spatio-temporal evolution of landscape ecology and urban function. Therefore, this study employs the megacity of Beijing as an example. It utilizes remote sensing and point-of-interest (POI) data spanning from 2008 to 2022 to construct an indicator system from two essential dimensions: urban form and function. We explored the spatio-temporal characteristics of alterations in urban expansion within the gradient buffer zone adjacent to the suburban railway network in Beijing. The results showed that: (1) The rates of urban expansion were highest in 2008–2013 and lowest in 2013–2018; moreover, suburban railways had the greatest impact on the built-up area within 2–4 km along the route, and the impact gradually decreased beyond 4 km. (2) The direction of urban expansion shifted northward in the direction of latitude and eastward in the direction of longitude from 2008 to 2022, with the shift in latitude being more distinct. (3) The number of urban functions gradually increased from 2008 to 2018, but the number of medical services suddenly increased and the number of other urban functions decreased from 2018 to 2022; in addition, urban functions other than scenic spots were mainly distributed in the main urban areas, with very few clusters distributed near stations. (4) The landscape shape index became more irregular and fragmented from the center along the route to the edge of the buffer zone from 2008 to 2013, and the degree of fragmentation was highest in the 2–4 km buffer zone. In summary, this paper analyzes the spatio-temporal characteristics of urban expansion along suburban railways through four indexes, namely expansion rate, expansion direction, urban function, and landscape shape, and the results of this study are of great significance to the development and planning of suburban railways in megacities.

Keywords: megacities; suburban railway; urban expansion; land cover; Beijing

Citation: Tang, H.; Yan, X.; Liu, T.; Zheng, J. Spatio-Temporal Evolution of Urban Expansion along Suburban Railway Lines in Megacities Based on Multi-Source Data: A Case Study of Beijing, China. *Remote Sens.* **2023**, *15*, 4684. https://doi.org/10.3390/rs15194684

Academic Editor: Yuji Murayama

Received: 31 July 2023
Revised: 10 September 2023
Accepted: 23 September 2023
Published: 25 September 2023

1. Introduction

With the acceleration of urbanization, China's urban population has experienced decades of rapid growth, and a number of megacities have emerged one after another. This has been accompanied by an overconcentration of population in urban areas, which puts increasing pressure on urban and regional transport systems [1]. As a swift and highly efficient mode of transportation, suburban railways assume a paramount role in alleviating traffic gridlock and expediting regional advancement [2,3]. Over the course of the previous two decades, virtually all of China's burgeoning metropolises have embarked on the expansion of their suburban rail transit systems. This is particularly evident in economically flourishing domains like the Yangtze River Delta and the Pearl River Delta [4]. Notably, even the recently proclaimed megacities of Chengdu and Wuhan, as of the conclusion of 2022, have set forth ambitious plans for the development of their own suburban rail transit

networks [5]. Therefore, the construction of suburban railways and urbanization promote one another, and studying the spatio-temporal characteristics of urban expansion along suburban railways is of great significance to the development and planning of suburban railways in megacities.

Urban expansion represents a form of land augmentation characterized by a lack of organization, low population density, and a monofunctional disposition in the trajectory of urban evolution [6]. As the twentieth century commenced, numerous scholars embarked upon the exploration of urban expansion [7]. In the domain of quantitative analysis, inquiries into urban sprawl, under the purview of geography and utilizing spatial analytical instruments [8,9], predominantly assess this phenomenon concerning land magnitude and spatial morphological attributes [10]. This approach juxtaposes variations in land cover, encompassing their quantity, typology, and geospatial distribution, in order to delineate the contours of urban expansion [11]. In recent years, with the innovation of the geographic information system (GIS) and spatial statistical techniques, the driving forces, prediction, and modeling of urban expansion have become hot research topics [12]. Several scholars have modeled the dynamics of land cover maps to find the driving forces affecting urban expansion in order to understand its dynamic mechanisms [13–16]. In addition, in terms of research methodology, scholars have also begun to analyze urban spatial structure characterization by combining spatial processing tools of remote sensing imagery and GIS with evaluation indicators in the analysis of urban expansion [17]. Currently, the most common evaluation indicators include urban expansion indicators and their derivatives (landscape indicators) under the impact of land cover transformation [18]. Urban expansion indicators, especially the rate of urban expansion, are a direct reflection of urban expansion to some extent [19]. Fragstats-based landscape indicators, such as patch shape index, landscape richness index, and landscape dominance index, are often used to explore urban patterns at different scales [20]. Despite the significant impact of the above studies on the field of urban expansion, most studies have focused on urban expansion processes within municipal boundaries, while urban expansion processes within the gradient buffer zones along suburban railways have rarely been examined, especially through the analysis of joint multidimensional urban expansion indicators.

Different from other modes of transport, suburban railways usually connect the core area of a city with its suburbs or satellite towns or even the entire metropolitan area, which, further to the city's mainline railways [21] and together with subways and light railways, constitute the rail transit system of megacities [22]. Since 1979, China has witnessed the emergence of eight megacities with global influence, such as Beijing, Shanghai, and Shenzhen, each with a population of more than 10 million in their central urban areas [23]. However, megacities transcend the dimensions of mere urban centers both in populace and in the intrinsic characteristics of their land cover and transportation modalities, a transformation attributed notably to the phenomenon of agglomeration [24–26]. It is imperative to underline that the land space composition pattern of China's megacities differs greatly from that of foreign metropolises [27]. The proportion of industrial land in China's megacities exceeds that of other cities [28,29]. As megacities progress beyond the industrialization phase and transition into an era defined by a service- and innovation-driven economy, the preeminent theme in urban land development transmutes from "expansion" to "convergence and agglomeration" [30,31]. Concerning the domain of transportation, the city influences regional mobility and resource distribution through the amalgamation of diverse land cover attributes. Transport facilities, in improving regional accessibility, at the same time counteract the selection of land properties, forming a "circular feedback mechanism" of transport and land cover [32], as well as a coupling relationship and interactive effects. From the related literature, we found that a large number of scholars have determined the significant impact of rail transit on urban structure form and function mainly through a variety of qualitative and quantitative methods [33,34]. Railway commuting constitutes a prevalent practice, particularly prominent in European nations such as the United Kingdom and Germany. During the latter decades of the preceding century, innovative concepts for the reconfiguration and repurposing of antiquated railway tracks,

coupled with the preservation of architectural treasures like bridges and tunnels within urban and suburban settings, were applied across various European domains [35]. As commuter patterns gravitate towards the periphery of urban areas, the emergence of novel expansion zones, often referred to as "sprawl," represents a transient phase within the continuous urban proliferation narrative [36,37]. It is worth mentioning that rail transit systems have an equally significant impact on the urban form and expansion process in megacities [38]. Compared with other cities, Beijing is one of the first megacities to plan and build suburban railways, and it is also one of the fastest growing cities in terms of suburban railways. The Beijing suburban railway is a realistic need for the development of the Beijing–Tianjin–Hebei metropolitan area to a certain stage, and it is also of great significance for the development of an integrated rail transit network to promote Beijing–Tianjin–Hebei synergy.

In summary, suburban railways are important connecting corridors that influence urban expansion and changes in regional patterns, so the focus of this paper is to investigate the regional expansion process of megacities affected by suburban rail transit systems, especially in a rapidly urbanizing country like China. Currently, many studies have considered the impact of rail transit on urban expansion. Nevertheless, the majority of these studies have directed their attention towards within the vicinity of railway stations or the internal urban structural elements, and very few have explored the evolutionary characteristics of urban expansion along suburban railways [2,4,39]. Therefore, this paper explores the regional impacts of suburban rail transit along suburban railways in Beijing, a megacity in China, as an example, and analyzes and compares the spatio-temporal characteristics of urban expansion along four suburban railway lines using multi-source remote sensing data over the time spans of 2008, 2013, 2018, and 2022. Combined with multidimensional analysis of urban expansion indicators, the spatio-temporal differences in expansion rate, expansion direction, urban function, and landscape indicators from the center along the railway to the edge of the buffer zone are explored, and the expansion characteristics within the gradient buffer zone along the railway are further analyzed. According to the needs of urban development, the integration of suburban lines as an integral part of the city needs to be realized [24]. Therefore, the findings of this paper are of great significance for the development and planning of suburban railways in megacities.

This study aims to address the following questions: (1) What are the characteristics of spatial and temporal differences in urban form under gradient buffer zones along suburban rail lines in megacities? (2) What are the characteristics of spatial and temporal differences in different urban functions under gradient buffer zones along suburban railways in megacities? The fundamental purpose is to explore the characteristics of urban expansion along suburban railways in megacities during China's rapid urbanization. This endeavor seeks to proffer valuable insight for urban planning and the adept administration of rail transit frameworks, fostering their synergetic coalescence with broader societal development paradigms.

2. Study Area

Beijing is the capital of China, a national central city, a megacity, a political center, a cultural center, an international communication center, and a science and technology innovation center [40]. As of 2020, Beijing had 16 districts under its jurisdiction, with a total area of 16,410.54 square kilometers. At the end of 2020, the resident population of Beijing was 21.893 million [41]. Beijing, located in the north of China, in the northern part of the North China Plain, and centered at 116°20′E longitude and 39°56′N latitude, is a world-famous ancient capital and modern international city [39].

With the rapid development of rail transit in China, suburban rail is also the focus of future urban rail transit construction in addition to intercity and urban rail. Taking Beijing as an example, this paper analyzes the spatio-temporal characteristics of urban expansion along suburban railways. As of February 2023, Beijing had four suburban railway lines in operation, including suburban railway line S1 (City Subcenter Line), suburban railway line S2, suburban railway line S5 (Huairou–Miyun Line), and suburban

railway line S6 (Tongzhou–Miyun Line), with a total mileage of 369 km and a total of 24 stations in operation within the city area. The lines covered nine municipal districts and one adjacent county, namely Miyun District, Huairou District, Shun District, Changping District, Yanqing District, Chaoyang District, Tongzhou District, Haidian District, Fangshan District of Beijing City, and Huailai County of Hebei Province [42].

In the course of the implementation of the Beijing suburban railway project, the years 2008, 2013, and 2018 marked significant milestones representing the commencement of construction, the commencement of operation, and the full operational phase of each suburban railway, respectively. Currently, China is in a period of rapid development, and a five-year interval is sufficient to reflect the evolving dynamics of urban land use. Therefore, this paper employed the years 2008–2013, 2013–2018, and 2018–2022 as the corresponding periods for construction, commissioning, and operation in this study. Detailed information is shown in Figure 1.

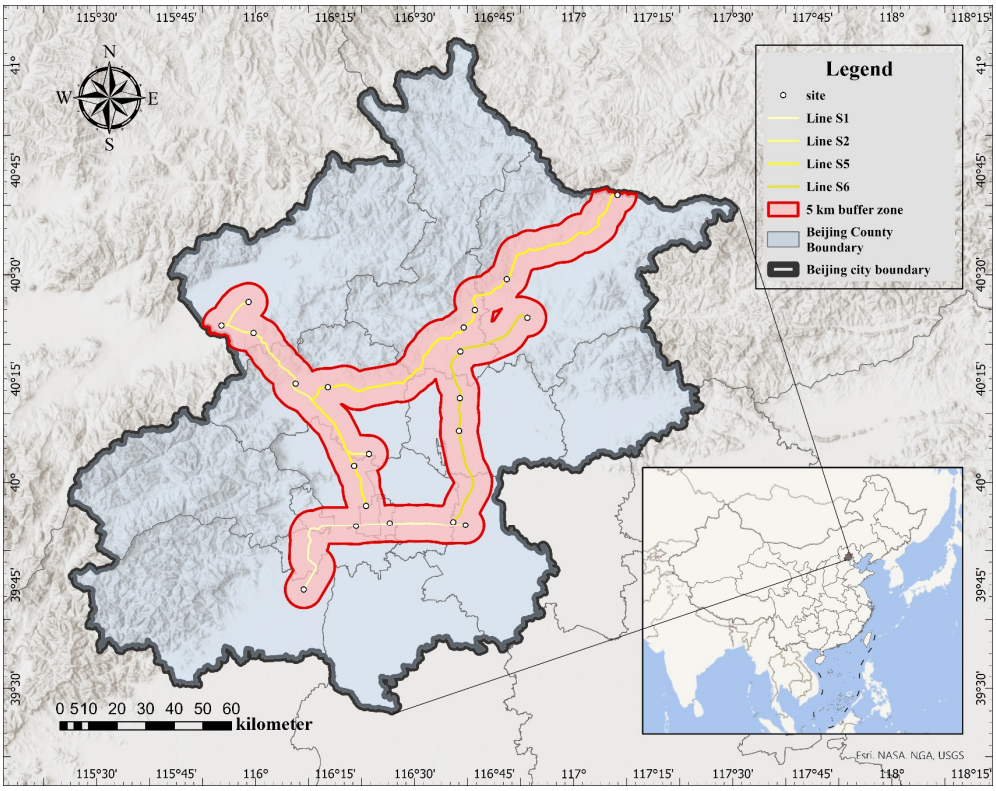

Figure 1. Study area.

3. Data and Methodology

3.1. Data

3.1.1. Data on Land Cover and Classification in Beijing

In order to study the spatio-temporal characteristics of the relationship between suburban railways and urban expansion in Beijing, this paper elucidates four important points in time to show their influential relationship. Firstly, remote sensing image data for the years 2008, 2013, 2018, and 2022 were obtained using satellites operated by the National Aeronautics and Space Administration (NASA) and the European Space Agency (ESA), as detailed in Table 1. Secondly, the 30 m resolution vector boundaries of Beijing were extracted from the National Basic Geographic Information Database, and the remote sensing images were preprocessed, fused, and spliced through the utilization of ENVI 5.3 software. A classification system was established based on the China Land Use Classification Standard (2022) and remote sensing images of current land use changes, which were mainly classified into arable land, forest land, grassland, watershed, building land, and unused land [43]. Thirdly, training samples from the study area using Google Earth were extracted separately

for supervised classification and visual interpretation to identify the land use types of Beijing in 2008, 2013, 2018 and 2022. Fourthly, kappa coefficients and overall accuracy were calculated based on the confusion matrix to evaluate classification accuracy. According to the classification results, the kappa coefficients for these four years were 0.92, 0.96, 0.95, and 0.96, with overall accuracies of 94.94%, 97.63%, 97.53%, and 97.40%. Finally, ArcGIS Pro software was utilized for editing operations to identify the land cover classification of Beijing (Figure 2).

Table 1. Information on land cover classification data in Beijing.

Type of Data	Year	Spatial Resolution	Data Sources	Remote Sensing Satellite	Format	Data Description
Remote sensing image data	2008 2013 2018 2022	15 m 10 m 10 m 10 m	NASA (https://www.nasa.gov, accessed on 20 December 2022) ESA (https://scihub.copernicus.eu, accessed on 7 January 2023)	Landsat-7 Landsat-8 Sentinel-2 Sentinel-2	Grid Grid Grid Grid	Obtaining Beijing land use data for calculating urban form expansion
Beijing Municipal Vector Boundary Data	2020	30 m	National Center for Basic Geographic Information (https://www.webmap.cn, accessed on 11 December 2022)		Vector	Including delineation of administrative areas and cropping of remotely sensed data

3.1.2. Other Basic Data

To explore the distribution of other basic data in Beijing, the following POI data were collected. First, Amap was used to obtain the data of each point of interest, such as medical services, science and education, scenic spots, and shopping services (Table 2), of which commercial services included shopping centers, general shopping malls, convenient supermarkets, etc.; science and education included schools, scientific research institutes, training institutes, etc.; medical services included general hospitals, sanitariums, pharmacies, etc.; and scenic spots included scenic spots, parks, city squares, temples, Taoist temples, etc. [44]. Second, Google Earth Pro software was used to obtain the data of 21 stations and 4 track lines of the Beijing suburban railway in 2022, which were saved as XML files. Finally, the data were imported into ArcGIS Pro software to carry out visualization and analysis.

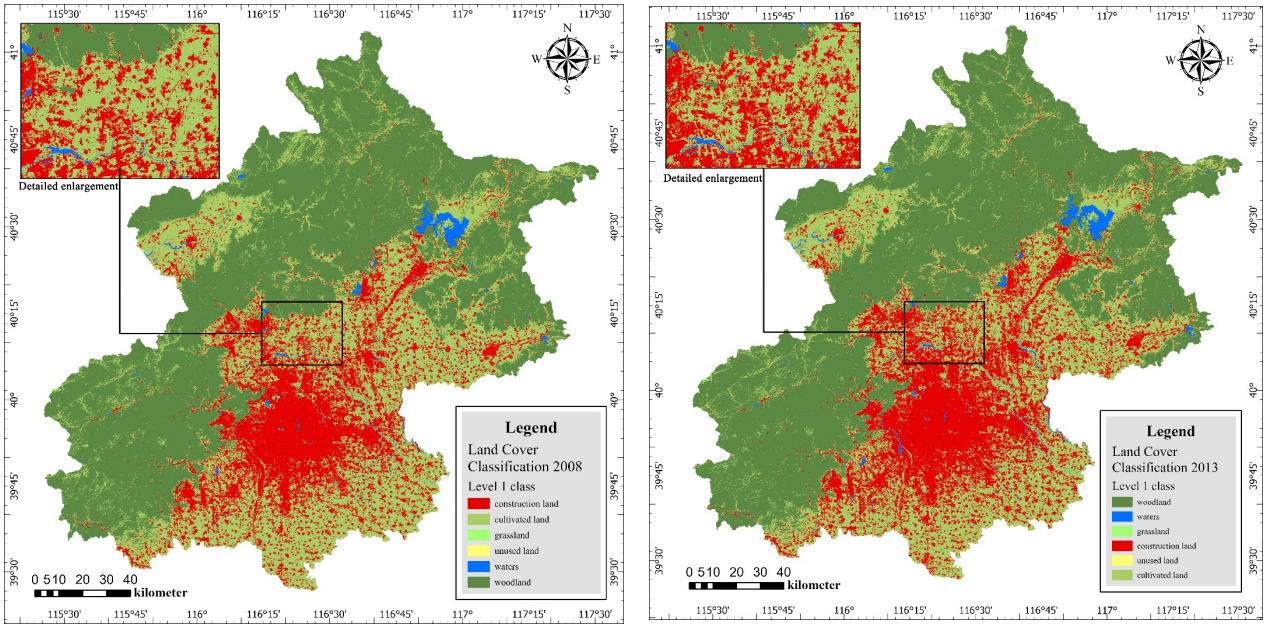

(**a**) (**b**)

Figure 2. *Cont.*

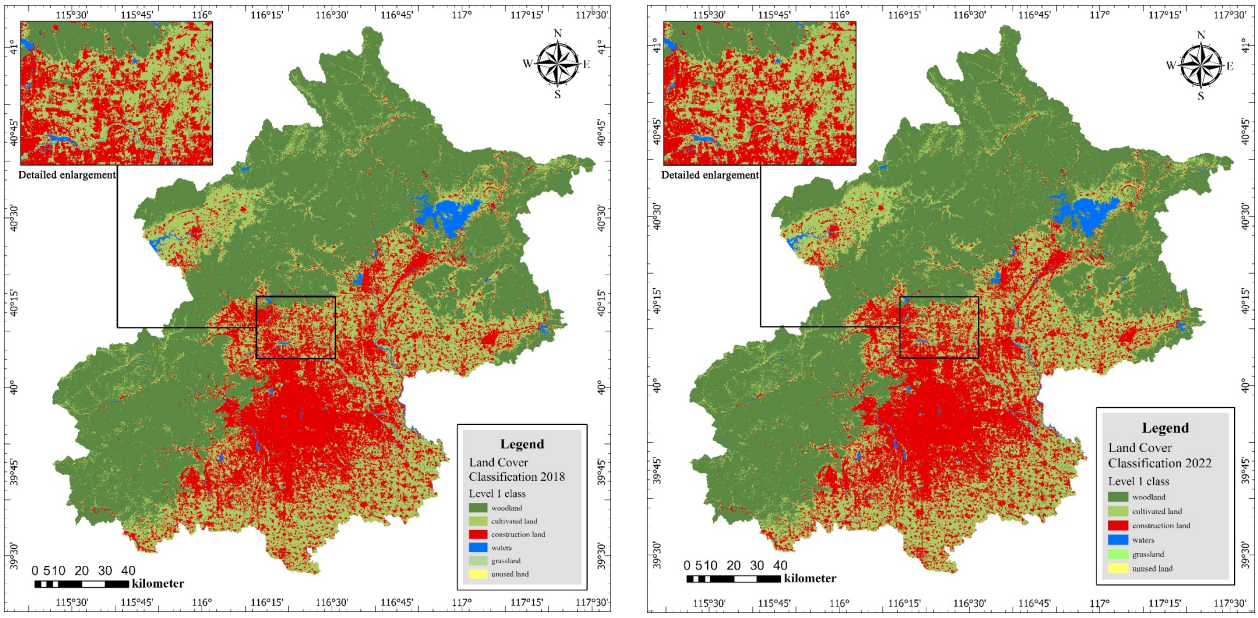

(**c**) (**d**)

Figure 2. Land cover classification map of Beijing at different periods. (**a**) Beijing land cover classification map in 2008; (**b**) Beijing land cover classification map in 2013; (**c**) Beijing land cover classification map in 2018; (**d**) Beijing land cover classification map in 2022.

Table 2. POI classification table.

POI Classification	Data Specificities	Data Sources
Medical services	Emergency Centers Disease Prevention Agencies Healthcare Service Sites Pharmacies Medical Clinics Specialized Hospitals General Hospitals	A map (https://lbs.amap.com, accessed on 6 March 2023)
Science and education	Museums Science and Technology Museums Art Museums Libraries Exhibition Halls Schools Training Organizations	
Scenic spots	Parks Zoos Botanical Gardens Memorials City Squares Temples and Churches Provincial Tourist Attractions	
Shopping services	Convenience Stores Comprehensive Markets Specialty Stores Shopping Malls Home Appliance and electronics Stores Home Building Materials Markets Specialty Shopping Streets	

3.2. Methods

The study was conducted in four steps. Firstly, it entailed comprehensive data preprocessing and establishment of the gradient buffer zone. Secondly, it developed a comprehensive indicator framework delineating urban expansion along the suburban railway, respectively in the dimensions of urban form (urban expansion rate, expansion direction, and landscape morphology) and urban function (medical services, science and education, culture, scenic spots, and shopping services). Thirdly, it identified the characteristics of spatio-temporal variations in urban expansion within the gradient buffer zone along the Beijing suburban railway. Finally, optimization strategies based on the above findings were discussed and proposed (Figure 3).

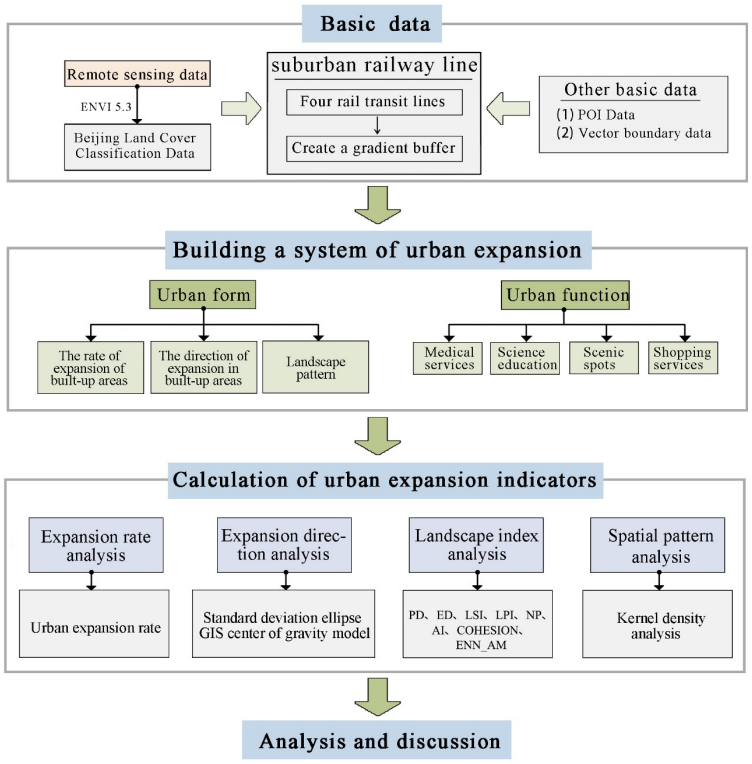

Figure 3. The flowchart of the research process [2,14,31,43,44].

3.2.1. Division of the Buffer Zone

According to the 2020 National Report of Commuting Monitoring in Major Cities, the average commuting time in major cities across the country is 36 min, with four megacities, including Beijing, having an average commuting distance of more than 8 km and an average commuting time of up to 40 min. This is due to the fact that the larger the city, the larger the spatial area over which commuting usually takes place and the commuting time increases [45]. It is worth mentioning that China introduced the concept of "living circle" in the 1980s, proposing a 15 min community living circle within the community and neighboring areas [46], thus dividing the city into 20 min basic living circles [47,48], and integrating the concept of living circle into the analysis of the accessibility of rail transit [49]. Among them, suburban rail transit in megacities was distinguished from urban rail transit by assuming the main transport link between the central city and the suburbs, and the average station distance was generally 2–5 km. Thus, this paper also distinguished the delineation of buffer zones along the route from the previous delineation with a fixed interval of 500 m. This was due to the fact that in past studies, walking scale was considered to be an important yardstick for the spatial layout and morphology organization of the site area and was the main reference for determining the influence circle and the scope of the plan [50–52]. However, with the development of society, residents have

become increasingly reliant on shared transport trips, and the planning of megacities has been dominated by large avenues and wide roadways, abandoning the earlier traditional community development patterns oriented to walking and public transit. Meanwhile, low-density, decentralized land cover patterns have led to a significant increase in shared electric bikes [53,54], but the vast majority of users are still focused on riding distances of less than 2 km [55]. Therefore, the pedestrian scale can no longer be used as the main reference for the delineation of suburban rail transit buffers [56,57]. In this study, in order to facilitate the description of the life radius of the impact domain along the railway lines, the suburban railway buffer zone was divided at a fixed interval of 2 km along the line on the basis of four buffer zones of 0–2 km (5 min riding distance), 2–4 km (10 min riding distance), 4–6 km (15 min riding distance), and 6–8 km (20 min riding distance) (Figure 4).

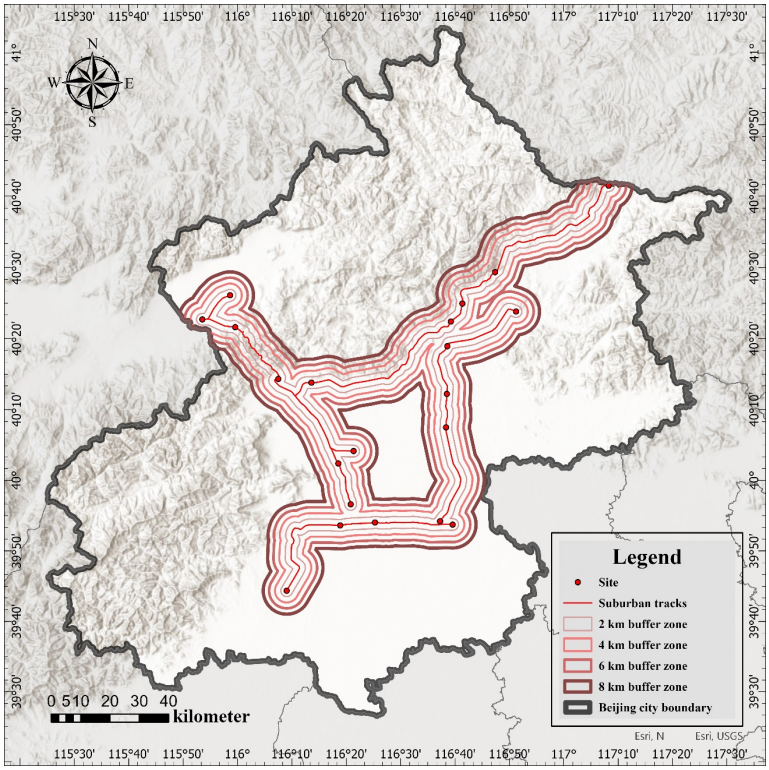

Figure 4. Schematic diagram of Beijing suburban railway stations and buffer zone delineation.

3.2.2. Analysis of the Spatio-Temporal Patterns of Urban Form Expansion

- Urban Expansion Rate (UER)

To examine the rate of urban expansion, we used the indicator of urban expansion rate (UER) [31]. The UER can be used to represent the change in urban area per unit of time during different periods of railway construction. This is a key indicator for evaluating spatio-temporal changes in urban expansion along rail transit routes. The UER is defined as follows:

$$UER_{\Delta T} = \frac{UA_{t+\Delta T} - UA_t}{UA_t} * \frac{1}{\Delta T} 100\% \quad (1)$$

where $UER_{\Delta T}$ is the urban expansion rate from time to time t; UA_t and $UA_{t+\Delta T}$ denote the urban area of the target unit at time t and the urban area at time $t + \Delta T$, respectively; and ΔT is the interval between study cycles (in years).

- Standardized Elliptic Difference

In order to further study the overall expansion direction and spatio-temporal trends of the built-up urban area, standard deviation ellipse analysis (SDE) was used. Based on the four-year urban built-up area within the buffer zone, SDE analysis allows for the calculation

of the four parameters of the weighted standard deviation ellipse, including the center of the ellipse, the long axis, the short axis, and the azimuthal angle. The long half-axis of the ellipse represents the direction of the data distribution and the short half-axis represents the range of the data distribution. The larger the difference between the values of the long and short half-axes (the larger the squash), the more pronounced the directionality of the data. Whereas the azimuth is determined as the angle of clockwise rotation of the long axis of the ellipse with the x-axis as the reference and due north as zero degrees, the change in azimuth indicates the degree of change in the directionality of the data [43]. The exact formulas are shown below:

$$\cos\theta = (A + B)/C \tag{2}$$

$$A = \left(\sum_{i=1}^{n} w_i^2 \overline{x}_i^2 - \sum_{i=1}^{n} w_i^2 \overline{y}_i^2\right) \tag{3}$$

$$B = \sqrt{\left(\sum_{i=1}^{n} w_i^2 \overline{x}_i^2 - \sum_{i=1}^{n} w_i^2 \overline{y}_i^2\right) + 4\left(\sum_{i=1}^{n} w_i^2 \overline{x}_i \overline{y}_i\right)^2} \tag{4}$$

$$C = 2\sum_{i=1}^{n} w_i^2 \overline{x}_i \overline{y}_i \tag{5}$$

$$\begin{cases} \overline{x}_i = x_i - \overline{x} \\ \overline{x}_i = y_i - \overline{x} \end{cases} \tag{6}$$

where θ is the orientation of the ellipse, indicating the angle to the long axis of the ellipse measured clockwise from north; $\overline{x}_i$ and $\overline{x}_i$ are the value of the deviation between the mean center and the center of the image element i, respectfully; and w_i is the weight. In this study, w_i means that the value x of the impervious surface fraction of the image element i and the standard deviation in the axial direction y are calculated according to the following equations:

$$\begin{cases} \sigma_x = \sqrt{\frac{\sum_{i=1}^{n} (w_i \overline{x}_i \cos\theta - w_i \overline{y}_i \sin\theta)^2}{\sum_{i=1}^{n} w_i^2}} \\ \sigma_y = \sqrt{\frac{\sum_{i=1}^{n} (w_i \overline{x}_i \sin\theta - w_i \overline{y}_i \csc\theta)^2}{\sum_{i=1}^{n} w_i^2}} \end{cases} \tag{7}$$

- GIS Center of Gravity Model

The center of gravity holds a pivotal role as a key metric in investigating urban expansion. It effectively illustrates the spatial and temporal distribution characteristics of construction land through the direction and distance of movement of the center of gravity. The direction and extent of the centroid's movement served as indicators of the magnitude of alteration and spatial disparities within the buffer zone over the three distinct time spans: 2008–2013, 2013–2018, and 2018–2022 [14,58,59]. The center of gravity model can accurately determine the spatial evolution of each element by measuring the spatial movement direction and geometric distance of the center of gravity position of each indicator. The center of gravity coordinates are calculated as follows:

$$X, Y = \left[\frac{\sum_{i=1}^{n} M_i X_i}{\sum_{i=1}^{n} M_i}, \frac{\sum_{i=1}^{n} M_i X_i}{\sum_{i=1}^{n} M_i}\right] \tag{8}$$

where (X, Y) is the center of gravity coordinates; X_i is the mass or weight of the plane i; X_i is the longitude or coordinates of the point i of the plane; and Y_i is the latitude or coordinates of the point i of the plane. In other words, (X, Y) is the geographic coordinates of the point i of the plane.

The direction of spatial movement of the center of gravity position, θ, in the year $t+1$ relative to the year t can be expressed as follows:

$$\theta = \theta_{t+1} - \theta_t = \left[\frac{k*\pi}{2} + \tan^{-1}\left(\frac{\overline{y}_{t+1} - \overline{y}_t}{\overline{x}_{t+1} - \overline{x}_t}\right)\right] * \frac{180^\circ}{\pi} \tag{9}$$

where $k = 0, 1, 2; \theta \in (-180^\circ, 180^\circ)$; east is 0°; and the counterclockwise direction is positive.

The center of gravity position is shifted by a geometric distance. The geometric distance of the center of gravity position of the year $t+1$ relative to the year t can be expressed as follows:

$$D = C * \sqrt{\left(\overline{x}_{t+1} - \overline{x}_t\right)^2 + \left(\overline{y}_{t+1} - \overline{y}_t\right)^2} \quad (10)$$

where C denotes the coefficient of conversion of the Earth's plane rectangular coordinates $(^\circ)$ into actual distance (km), taking the value of 111.111.

- Landscape Metrics

In this paper, Fragstats 4.2 software was used to calculate and de-correlate several landscape indices that characterized the landscape shape changes in this study area. Finally, eight landscape indices were selected to describe the urban expansion pattern along the Beijing suburban railway: patch density (PD), edge density (ED), landscape shape index (LSI), largest path index (LPI), patch-type cohesion index (COHESION), number of patches (NP), aggregation index (AI), and area-weighted mean Euclidean nearest neighbor distance (ENN_AM). Three of these landscape metrics were used to determine the stage of urban expansion, including patch density (PD), edge density (ED) and area-weighted mean Euclidean nearest neighbor distance (ENN_AM) [2]. Through the collation of related literature, it could be seen that the selection of the above indicators to characterize the urban expansion pattern along the Beijing suburban railway was based on the following:

The PD value is expected to increase during rapid growth of built-up urban areas, but may decrease if urban areas merge into a continuous urban fabric. The ED value is used to reveal the extent to which a landscape or type is divided by boundaries, and is a direct response to the degree of landscape fragmentation, with higher boundary densities reflecting higher landscape fragmentation. The LSI metric is a measure of landscape shape complexity, and LSI increases with shape irregularity. The LPI metric provides the total area occupied by the largest parcel as a percentage of the built-up area of the city, and will equal 100 when the entire landscape consists of a single patch. Given that cohesion (COHESION) is a measure of physical connectivity, the cohesion index increases over time, indicating that urban patches are more physically connected to subway construction. NP is the total number of patches of a given type contained in the landscape as a whole, and the number of patches is, to some extent, a measure of the degree of fragmentation of that particular patch type. The AI metric only considers similar adjacencies involving the focal classes, not adjacencies to other patch types. Maximum AI is achieved when the patch type consists of a single compact patch [44,60–64]. This paper pre-analyzed the changes and significance of the landscape index of the built-up areas within the Beijing suburban rail gradient buffer zone in 2008, 2013, 2018, and 2022 through the calculation results of the above landscape indexes, and correlated the value of each landscape index with the corresponding amount of urban expansion in the buffer zone.

3.2.3. Analysis of Spatio-Temporal Patterns of Urban Functional Expansion

POI data can reflect the level of urban functioning in an area over time [65]. In order to explore urban functioning over time, this study used the kernel density method to map spatial and temporal changes in urban functioning. Kernel density analysis utilizes a kernel function to calculate the density of the area surrounding the POI point elements and calculates the degree of clustering of the point elements throughout the study area based on the overall element input, resulting in a continuous density surface in the plane [34]. This method yielded the spatially distributed aggregation area of the four types of POI data within the 8 km buffer zone of the suburban railway for the years 2008–2022, and the kernel density calculation formula is shown below:

$$f_n(x) = \frac{1}{nh^2\pi} \sum_{i=1}^{n} K\left[\left(1 - \frac{(x - x_i)^2 + (y - y_i)^2}{h^2}\right)\right]^2 \quad (11)$$

where $f_n(x)$ is the kernel density value; K is the kernel function; x_i and y_i denote independently distributed number i of sample points; $(x - x_i)^2 + (y - y_i)^2$ is the distance between the sample points (x_i,y_i) and (x, y); h is the bandwidth; and n is the number of points in the sample range.

4. Results

4.1. Spatio-Temporal Characteristics of Urban Formation Expansion along the Beijing Suburban Railway

4.1.1. Rate of Urban Expansion in the Buffer Zone

Figure 5 illustrates the rate of urban expansion within various buffer zones along the Beijing suburban railway during three distinct time intervals: 2005–2013, 2013–2018, and 2018–2022. Remarkably, all three curves exhibited a gradual crescendo, peaking within the 2–4 km buffer zone. After reaching the peak, the rate of urban expansion experienced a reduction as the distance from the suburban railway increased. Within each different buffer zone, UER attained its zenith between 2008 and 2013. This indicated that during the planning phase, the Beijing suburban railway exerted the most substantial influence on the pace of urban expansion. Notably, this influence was more pronounced in the 2018–2022 period than in the 2013–2018 period.

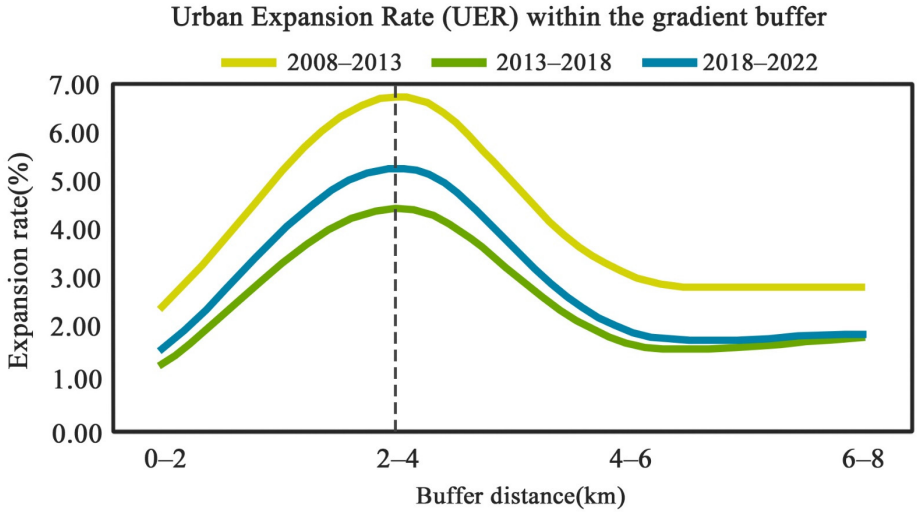

Figure 5. Urban expansion rate (UER) for different time periods within each buffer zone of the Beijing suburban railway (BSR).

Figure 6 shows the process of built-up area expansion within different buffer zones. Between 2008 and 2013, land cover along the Beijing suburban railway underwent significant changes. However, there were significant differences in the characterization of spatial expansion within different buffer zones. For example, in Figure 5, the process of urban expansion can be clearly observed within the 2–4 km buffer zone of the suburban line. New urban built-up areas were concentrated around some of the stations within a 2–4 km buffer zone. Within the 4–6 km buffer zone, additional urban built-up areas were also located mainly in the vicinity of the site but were relatively dispersed. In addition, the process of urban expansion was virtually independent of the administrative boundaries of the 2–4, 4–6, and 6–8 km buffer zones of the peri-urban routes. Within these buffer zones, the distribution of new urban areas occurred not only in the city center but also in the suburbs, indicating that urban expansion areas significantly impacted by suburban railway lines were located within the 2–4 km buffer zone along the railway. When the distance to the buffer zone along the railway was more than 4 km, the impacts became smaller and irregular.

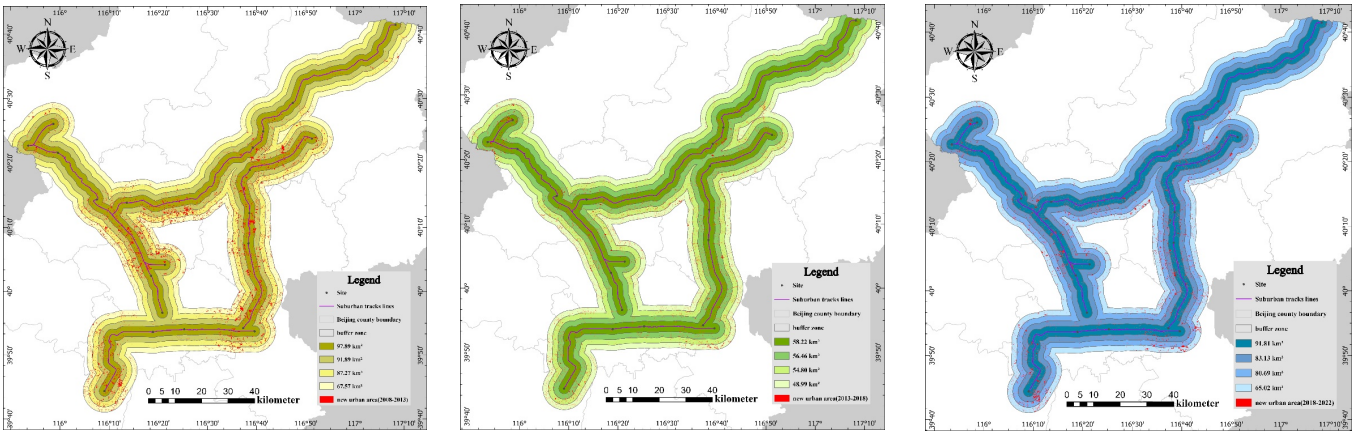

(**a**) (**b**) (**c**)

Figure 6. Expansion of built-up areas within different buffer zones of the Beijing suburban railway (BSR). (**a**) Expansion process in 2008–2013; (**b**) Expansion process in 2013–2018; (**c**) Expansion process in 2018–2022.

4.1.2. Direction of Urban Expansion within the Buffer Zone

From Table 3 and Figure 7, it can be seen that the standard deviation ellipse area of the urban built-up area within the 8 km buffer zone of the Beijing suburban railway increased from 2008 to 2022. The standard deviation ellipse area had the highest growth of 88.90508 km^2 between 2013 and 2018, followed by 73.655233 km^2 between 2008 and 2013, and the least growth of 64.110655 km^2 between 2018 and 2022. The growth was more significant in the long-axis direction and only slight in the short-axis direction. In addition, the azimuthal turn angle did not change much between 2008 and 2022, basically remaining at about 51°. The long axis of the standard deviation ellipse of the urban built-up area within the 8 km buffer zone of the Beijing suburban railway remained the same in the past 14 years, which developed along the southwest to northeast direction, and the spatial distribution of the urban built-up area of Beijing basically presented this pattern.

Table 3. Changes in standard deviation ellipse parameters for built-up land within the 8 km buffer zone of the Beijing suburban railway, 2008–2022.

Land Cover Type	Year	Longitude of Center of Gravity (°)	Latitude of Center of Gravity (°)	Long Axis (km)	Short Axis (km)	Area (km^2)	Azimuthal Angle
Built-up land	2008	116.4683785°	40.2179009°	54.097	37.296	6338.313251	50.546086
	2013	116.4729132°	40.2283607°	54.825	37.228	6411.968484	51.166139
	2018	116.4734047°	40.2372073°	54.944	37.658	6500.087356	52.967368
	2022	116.4756533°	40.2417699°	54.971	37.636	6564.198011	53.791791

From Table 4 and Figure 8, it can be seen that the center of gravity of the standard deviation ellipse of the urban built-up area within the 8 km buffer zone of the Beijing suburban railway from 2008 to 2022 showed a localized shift, with the direction of latitude moving to the north and the direction of longitude moving to the east. From 2008 to 2013, the coordinates of the center of gravity of the built-up area shifted from (116.4683785°, 40.2179009°) to (116.4729132°, 40.2283607°), with the center of gravity shifting by 1.61 km at an angle of about 108.43°, moving in a northeast direction at a rate of 322 m/year, with a greater distance of shift. Between 2013 and 2018, the coordinates of the center of gravity of the built-up area shifted from (116.4729132°, 40.2283607°) to (116.4734047°, 40.2372073°), which was a shift in the center of gravity of 1.29 km at an angle of about 92.54° and a rate of 258 m/year. Both the offset distance and offset angle were reduced compared to between 2008 and 2013. Between 2018 and 2022, the coordinates of the center of gravity of

the built-up area shifted from (116.4734047°, 40.2372073°) to (116.4756533°, 40.2417699°), which was a shift in the center of gravity of 0.71 km at an angle of about 110.44° and a rate of 178 m/year. In summary, it can be seen that the urban built-up area within the 8 km buffer zone of the Beijing suburban rail had the fastest offset speed and farthest offset distance from 2008 to 2013, followed by 2013 to 2018, and the slowest offset speed but largest offset angle from 2018 to 2022.

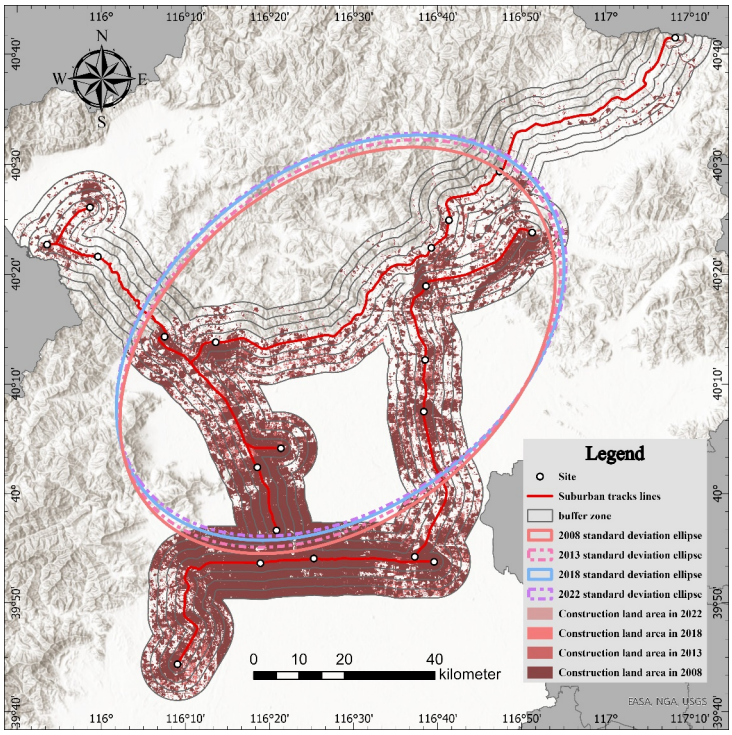

Figure 7. Standard deviation ellipse analysis of built-up land.

Table 4. Changes in the center of gravity of built-up land within the 8 km buffer zone of the Beijing suburban railway, 2008–2022.

Land Cover Type	Year	Clockwise and Eastward Angle	Offset Distance (km)	Offset Speed (m/year)
Built-up land	2008–2013	108.43°	1.61	322
	2013–2018	92.54°	1.29	258
	2018–2022	110.44°	0.71	178

4.1.3. Landscape Gradient Analysis along Beijing Suburban Railway

Figure 9 shows the changes in landscape indicators within the gradient buffer zone along the Beijing suburban railway. The indicators for these four buffer segments were calculated using the 2008, 2013, 2018, and 2022 urban built-up areas. It can be clearly seen that four of the indicators (PD, ED, LPI, and AI) showed decreasing trends year by year in 2008, 2013, 2018, and 2022, with the most obvious fluctuation in the ED value and more moderate fluctuations in the other values, as shown in Figure 9A,B,D,H. Meanwhile, two indicators, LSI and COHESION, showed increasing trends from year to year, but the COHESION index decreased with the expansion of the buffer zone range, as shown in Figure 9C,E.

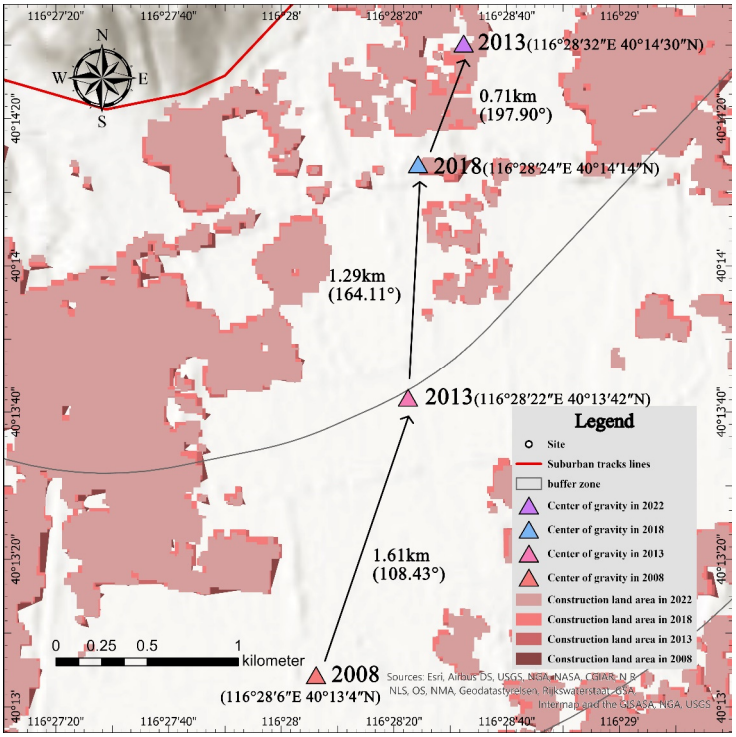

Figure 8. Shift in center of gravity analysis of built-up land.

Prior to the construction of the Beijing suburban railway (BSR), the 6–8 km buffer zone in 2008 had the highest PD index (Figure 9A). This indicator decreased significantly during the route planning period, but the overall trend in this indicator was an increase with distance from the buffer zone. In 2022, the PD index was less in all buffer zones, with the 0–2 km buffer zone have the lowest value, and this index described the pattern of aggregation of patches under the gradient buffer zone.

In terms of the ED index (Figure 9B), the degree of boundary of built-up patches generally showed a decrease with buffer zone distance, with the index being highest in 2008 and decreasing over time, but the overall fluctuation in this value was the most significant.

The change in LSI illustrated the low complexity of the shape of the built-up area of the city center within the gradient buffer zone along the suburban railway. As shown in Figure 9C, the peak of LSI occurred in 2022. The LSI index for each buffer segment gradually increased from 2008 to 2022. This meant that as cities expanded, urban area patches became increasingly complex, especially within the 2–4 km buffer zone along the railway.

The LPI values (Figure 9D) for 2008, 2013, 2018, and 2022 were all highest and varied slightly within the 0–2 km buffer zone, and were lowest and generally fluctuated moderately in the 6–8 km buffer zone. There was also a trend of decreasing LPI values from year to year within the gradient buffer zone.

The COHESION values increased over time, indicating that urban patches were more physically connected to railway construction. As can be seen in Figure 9E, COHESION values were lowest in the 6–8 km buffer zone in 2008 and approached 100 in the 0–2 km buffer zone in 2022, which indicated aggregated characteristics along the gradient buffer zone after the suburban line was put into operation.

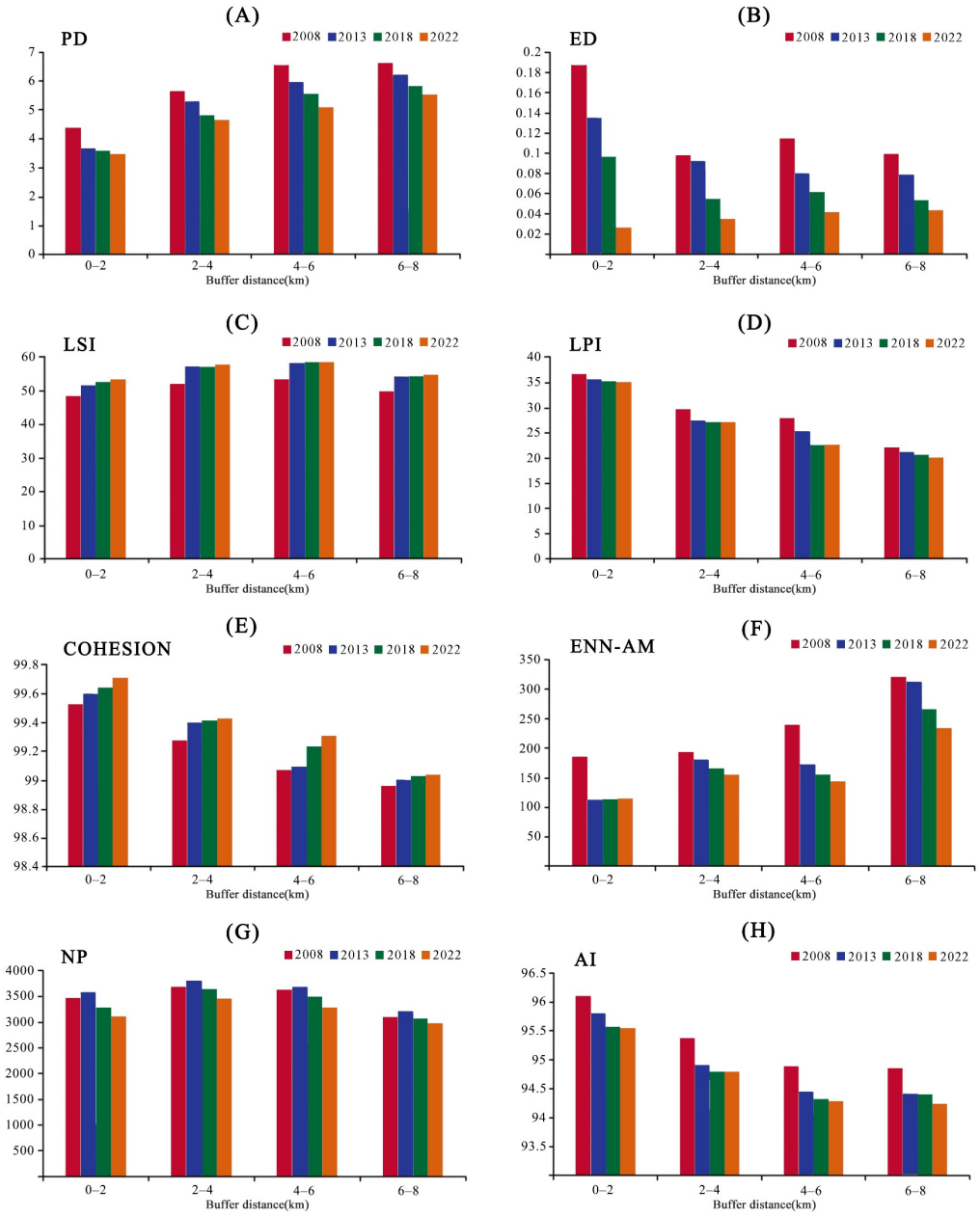

Figure 9. Changes in landscape indicators of the gradient buffer zone along the Beijing suburban railway.

Changes in the ENN-AM index (Figure 9F) within the gradient buffer zone of the Beijing suburban railway (BSR) revealed the degree of agglomeration from along the tracks outward. The ENN-AM values in the 2–4 km buffer zone no longer decreased after line construction, indicating that the urban built-up areas were increasingly clustered along suburban railways as the city expanded.

As can be seen from Figure 9G, the degree of fragmentation of built-up area patches decreased with the expansion of buffer distance, with the highest NP index in the 2–4 km buffer zone, but the overall fluctuation trend was not obvious. It is worth noting that the NP index was highest in 2013 even under the gradient buffer zone.

From the AI index (Figure 9H), it can be seen that the degree of agglomeration gradually decreased with time; the index was minimized in the 6–8 km buffer zone, and the index peaked in the 0–2 km buffer zone. However, the fluctuations in the decrease in this index with increasing buffer zone distance were more moderate.

4.2. Spatio-Temporal Characteristics of Functional Expansion of Cities along Beijing Suburban Railway

4.2.1. Analysis of the Number of Urban Functions in the Buffer Zone in Terms of Percentage

According to Figure 10, the numbers of these four urban functions (shopping services, science and education, medical services, and scenic spots) within the 8 km buffer zone along the Beijing suburban railway can be seen in terms of the changes in the number and proportion in each year. Of these, the urban function of scenic spots increased most slowly and steadily over the four years, remaining at about 3% of the total. Similarly, the number of science and education facilities continued to increase, but the proportion fluctuated slightly, from 36% in 2008, then dropping to 21%, then rising again to 24% and finally stopping at 14%. Although the number of shopping services showed the most significant increase, at the same time, the proportion of this function was inversely related to that of the medical services function between 2018 and 2022, and the proportion of shopping services peaked at 64% in 2013 and eventually decreased to a minimum of 31% in 2022. It is worth noting that the number of medical services increased dramatically and reached 161,889 in 2022; furthermore, this urban function increased at a much faster rate than any other urban function and accounted for 53%, more than the sum of the other three urban functions.

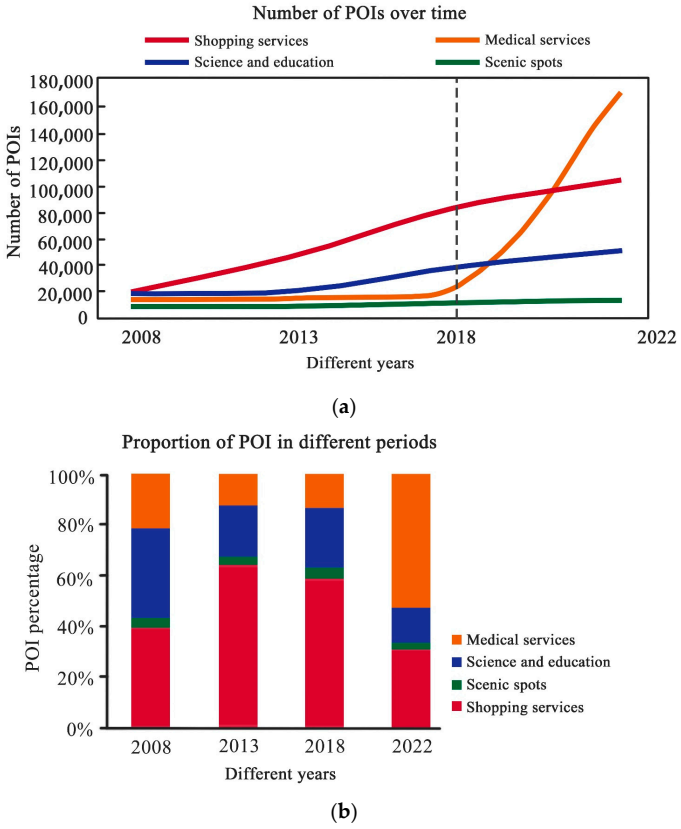

Figure 10. POIs in the Beijing suburban railway buffer zones in different periods (**a**) Number of POIs (**b**) POI percentage.

4.2.2. Analysis of the Spatial Distribution of Urban Functions in the Buffer Zone

Based on the kernel density plots for the four urban functions under each year in Figure 11, it can be seen that:

(1) From the POI total kernel density map within the 8 km buffer zone of Beijing suburban railway in 2008, 2013, 2018, and 2022, the main urban area was centered on the intersection of the Huairou–Miyun Line and the urban sub-center line with a high density of spatial distribution and clear structural hierarchy. The city center radiated east to the West Tongzhou–Miyun Station of the Tongzhou–Miyun Line and north to the Huangtudian Station of the S2 Line. Several other high-density clusters were more randomly located but were also in close proximity to the stations;

(2) Comparing the temporal development of these four urban functions, it can be seen that the numbers of all four urban functions gradually increased from 2008 to 2018. While the number of shopping services was always the highest, the number of medical services increased sharply and suddenly from 2018 to 2022, while the numbers of the other three urban functions decreased to varying degrees;

(3) Comparing the spatial development of these four urban functions, it can be seen that the expansion of the urban function of shopping services was more rapid and the radiation was more obvious, while the function of science and education showed the opposite trend. From the perspective of spatial distribution, the distribution of the three urban functions other than scenic spots was mainly in the main urban areas, with very few clusters distributed near stations and the urban functions of shopping and medical services being the most significant. Densities along the railways were highest in the 2–4 km buffer zone and lowest in the 6–8 km buffer zone.

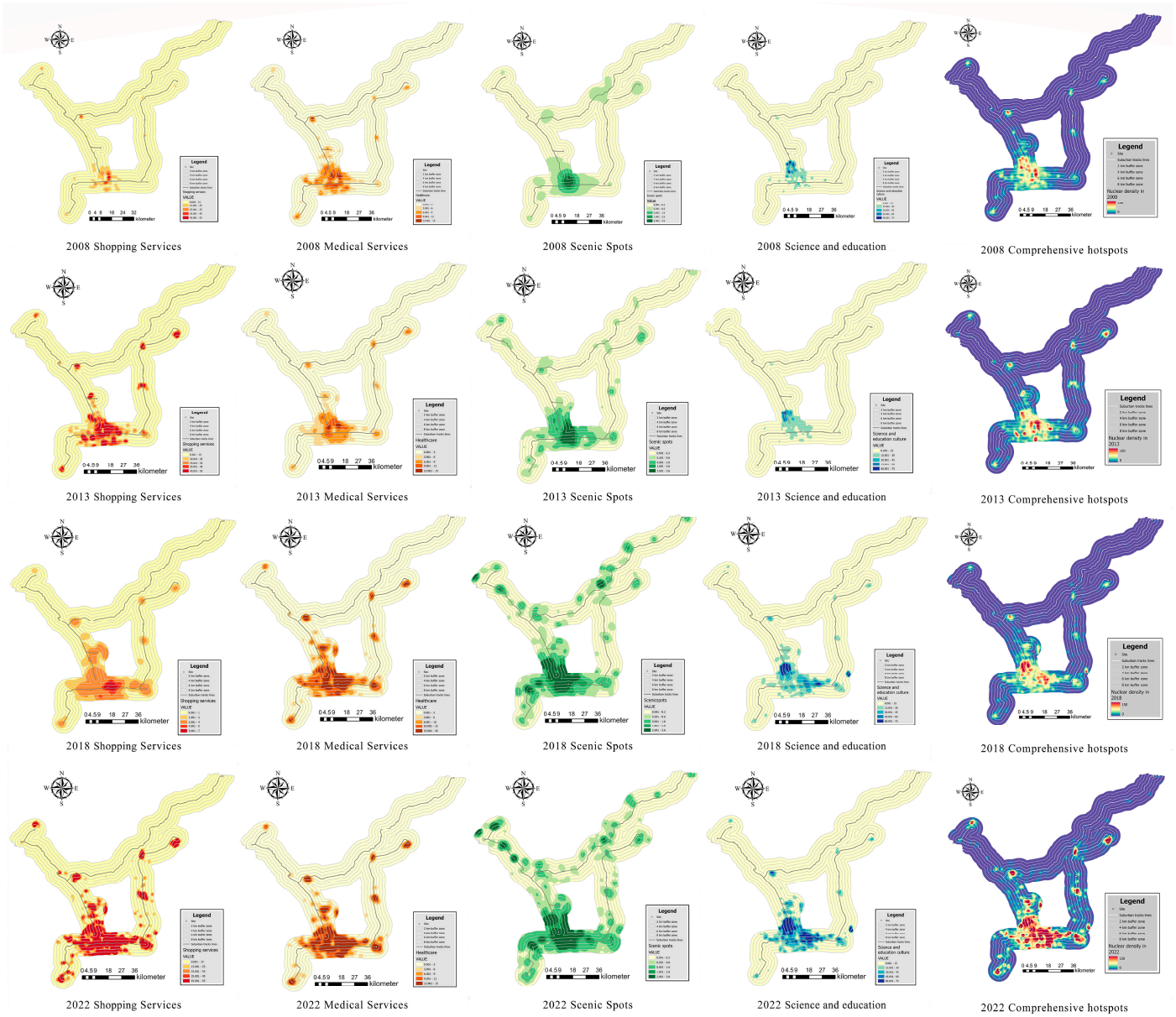

Figure 11. Density analysis of different types of POI distribution in the 0–8 km buffer zone of Beijing suburban railway at different times.

5. Discussion

5.1. Quantification of Urban Expansion along Suburban Railways

At present, the center of gravity of China's urban development has gradually shifted from the central area with high development density to the suburbs, and the pressure of the "single core" in the central area of large cities, especially megacities, urgently needs to be relieved [15]. Rapid population and economic growth in megacities has driven urban expansion and made urban land cover more intensive and efficient. Therefore, it is difficult to identify problems with urban expansion if it is quantified solely on the basis of urban conditions [66]. As megacities will face greater land supply difficulties and environmental constraints, more efficient and highly targeted transport system standards should be formulated. Suburban railways are an important means of transport between urban centers and their surrounding towns and cities, so it is particularly important to study the spatio-temporal dynamics of urban expansion along suburban railways. However, quantifying such a complex spatio-temporal process is a challenge. Our study establishes a framework of urban expansion indicators and landscape metrics to quantify the spatio-temporal evolution of urban expansion along suburban railways in megacities.

The system of indicators in this study was based on the core connotation of urban expansion along suburban railways, which was carried out in two dimensions: urban form and function. In previous literature on the spatio-temporal characteristics of urban expansion, most studies analyzed two dimensions: urban form and landscape shape. Among them, the rate and direction of urban expansion are the two most commonly used indicators to characterize the evolution of urban spatial form [67], and these indicators are used to calculate urban spatial form characteristics such as shape, agglomeration, and compactness [68]. The evolution of the spatial form of a city can clearly portray the advancement of urbanization and also affect the sustainable development of the city [69]. Landscape shapes include patch density (PD), edge density (ED), and area-weighted mean Euclidean nearest neighbor distance, which quantify the degree of fragmentation of the urban landscape [45]. It is worth mentioning that combining landscape metrics with gradient analysis can better characterize the complex spatial dynamics of urban expansion along transport corridors [4], and this paper needed to take into account the special characteristics of suburban railways. Therefore, density studies of urban functions were included, and urban expansion was characterized by low density or a tendency for density to decrease over a period of time [70]. For the choice of data type, we used POI data from electronic maps to reflect the distribution of urban functions. The density distribution of POIs can be used to effectively identify urban boundaries and explore the impact of different land cover attributes along transport corridors [71,72]. Meanwhile, in order to minimize the overlap between various urban functions and to facilitate analysis of the refined urban function forms and their expansion, this paper finally selected four categories of urban function for the analysis of urban expansion along suburban railways [30].

In summary, due to geographic conditions, spatial distance, and development stage, urban expansion within the gradient buffer zone along the Beijing suburban railway presented different spatial development characteristics. Therefore, the selection of multi-dimensional urban expansion indicators and the multi-scale scope of the study enabled a more significant analysis of the spatio-temporal characteristics of urban expansion along suburban railways.

5.2. Urban Expansion along Suburban Railways

Global experience has shown that growing megacities also often experience significant changes in their functional and spatial patterns [73], especially in China's megacities [74]. It has been demonstrated that urban expansion increases the demand for transport to the urban fringe, while improved transport conditions will in turn affect the city by enhancing the accessibility of the urban fringe, which in turn triggers the evolution of the land-use structure and promotes faster outward development of the city [75]. Therefore, this study

analyzed the spatio-temporal characteristics of urban expansion along suburban railways, using the megacity of Beijing as an example.

In this study, we used various indicators to measure the spatio-temporal pattern of urban form expansion along suburban railways under different time periods, which is important for examining the temporal effects of suburban railways. According to the results, urban expansion within the buffer zone along the Beijing suburban railway line reached its highest rate in 2008–2013 and had the greatest impact on the area between 2 and 4 km of the lines, while the urban patches became more complex, irregular, and dispersed. From 2013–2018, urban expansion rates were lowest along the railway lines, but the numbers of urban functions continued to rise in all four categories. In addition, the fragmentation of the urban area was highest in the 2–4 km buffer zone and decreased to a minimum in the 6–8 km buffer zone. Unlike railway systems in other countries, China's suburban railways are predominantly the result of transforming the existing historical railways, characterized by wider tracks and at-grade intersections with the surrounding land; in contrast, subways are mostly based on underground transportation [76].

Compared to urban rail transit systems such as subways and light rails, suburban railways wield a substantially more extensive spatial influence. While the typical metro line stretches less than 50 km in length, suburban rail lines span from 50 km to 100 km onwards. This is coupled with more extensive distances between stations; the average inter-station spacing on suburban rail lines greatly surpasses that of subways, typically ranging from 2 to 5 km, as opposed to the 1 km average seen in subways. Furthermore, they boast higher transport capacity [22,77]. As a consequence, the construction process necessitates larger areas for isolation and buffering. The convergence of ecological corridors with suburban railways creates ecological breakpoints, severely impeding species migration and dispersion [78]. As evident in Figure 12, protective isolation nets are prevalent along the Beijing suburban railway, which have a significant effect on urban development and landscape ecology. Consequently, this leads to a notable degree of landscape fragmentation within the 2–4 km buffer zone. Furthermore, the reduced rate of Beijing's urban expansion also impacts the extent of urban fragmentation. The research results showed that the fragmentation rate decreased to the lowest level within the 6–8 km buffer zone along the route, consistent with previous research findings [79]. The number of city functions other than health care declined from 2018–2022. At the same time, it could be observed that significant changes in urban functioning occurred in the vicinity of the stations, rather than in the city center. This was due to the fact that the demand for suburban rail transit influences urban planning along railways, which in turn guides urban expansion around suburban rail stations [4]. Throughout the study period, the direction of urban built-up area expansion shifted northward in the latitudinal direction from 2008 to 2022 and the shift was more pronounced. It is worth noting that the southern part of Beijing is highly developed, and the area that has space to further develop in the future is the north [80]. This was consistent with the construction direction and operation time of the Beijing suburban railway, indicating that the spatio-temporal characteristics of urban expansion in the built-up areas along the suburban railway showed a close relationship with its development and construction.

Second, this paper characterized the spatio-temporal features of urban expansion within the suburban railway buffer zone in terms of function by conducting a density study of urban function. It is worth noting that the POI data for 2018–2022 showed a significant change from the previous two periods, for which the global COVID-19 outbreak since the end of 2019 needs to be taken into account for the sudden increase in the number of medical services in the buffer zone along the railway (Figure 13). According to epidemiological data, local public policies such as social distancing initiatives, the use of masks, and economic blockades played a decisive role in the control of COVID-19 [80], while cases generated through public transport played an important role in the transmission of COVID-19, and connectivity and distance between infected areas and destinations were important determinants of transmission risk [81]. Therefore, the shutdown of suburban railway lines

undoubtedly created a huge resistance to social development during the epidemic, which ultimately led to a decline in the number of functions of the city, except for the health care function. During the period when the Beijing suburban railway lines were out of service, the number of scenic spots and attractions within the buffer zones along their routes declined slightly and fluctuated slightly, while the number of shopping services declined the most, followed by science and educational facilities, a phenomenon that cannot be ruled out due to the retreat of the real economy and launch of the "double reduction" policy in recent years. With the implementation of the "double reduction" policy, all regions of the country are actively exploring new modes of public service provision for compulsory education in this context, especially in the form of after-school services; however, the lack of effective guidance from the government to out-of-school training institutions [82] and other factors ultimately led to a decline in the functions of culture and education.

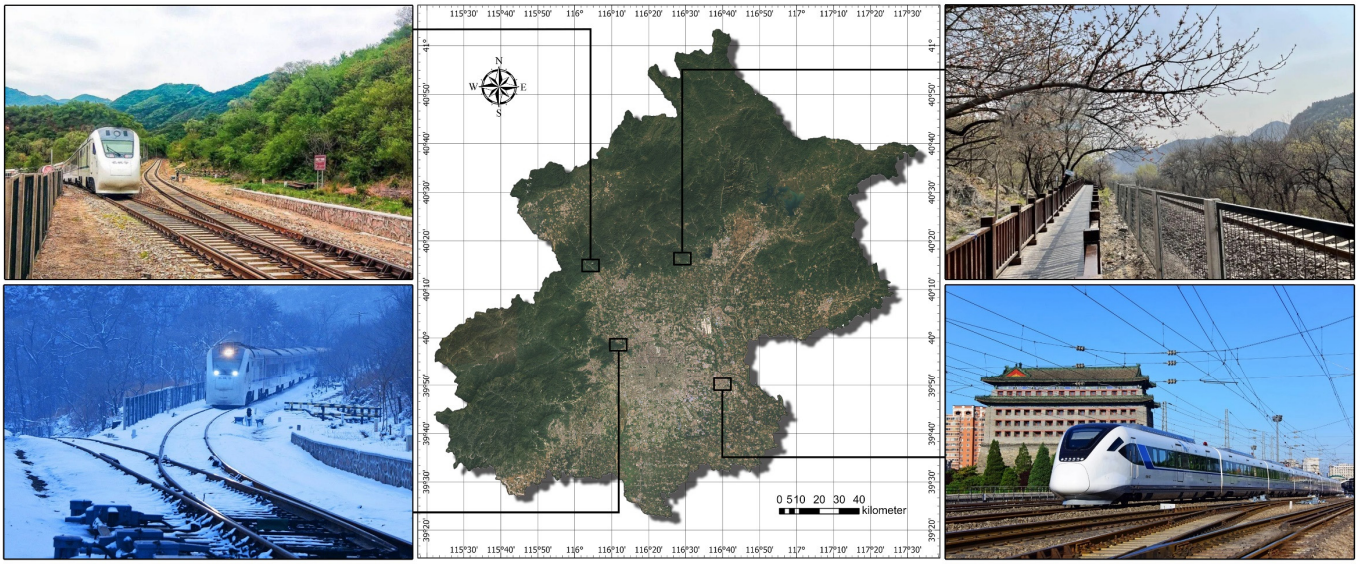

Figure 12. Current status node map of the Beijing suburban railway.

In response to the spatio-temporal characteristics of the urban expansion of the Beijing suburban railway, as mentioned above, the following development strategies are proposed: (1) Construct suburban railway ecological corridors since the suburban railway, as an artificial corridor, has caused the fragmentation of the regional landscape's ecological pattern, which affects regional ecological security. The construction of a green transport corridor coordinated with the ecological and social environment of the road area, and good greening and protection projects of the suburban railway have great significance for the enhancement of the spatial planning of the suburban railway [83]. (2) An information network space can be established by means of traffic centered at functions for urban spatial planning. Future rail transit stations will become the basic spatial unit of the organization of information flow convergence and decision-making management; entity, virtual body functional elements, and flow space in the "basic network + multiple nodes" can re-direct information convergence. Whether culture and leisure, eco-tourism, or government service functions, a reasonable division of labor and organic interaction between the center and periphery should be realized on the basis of the polycentric geospatial structure of "network + nodes" [84]. (3) Coordinate the development of suburban railways with intercity rail transit. In order to build an efficient and open integrated comprehensive transport system, the construction of intercity and suburban rail transit networks can be planned in an integrated manner. From the extent of the center of gravity shift in Beijing's built-up area and its development status, some provincial areas around Beijing have developed factual commuter demand. In the future, Beijing's urban, comprehensive transport, and rail transit network planning must focus on the trans-regional metropolitan

area [85], forming a land development and suburban rail transit-guided urban development pattern that is conducive to the development of public transport.

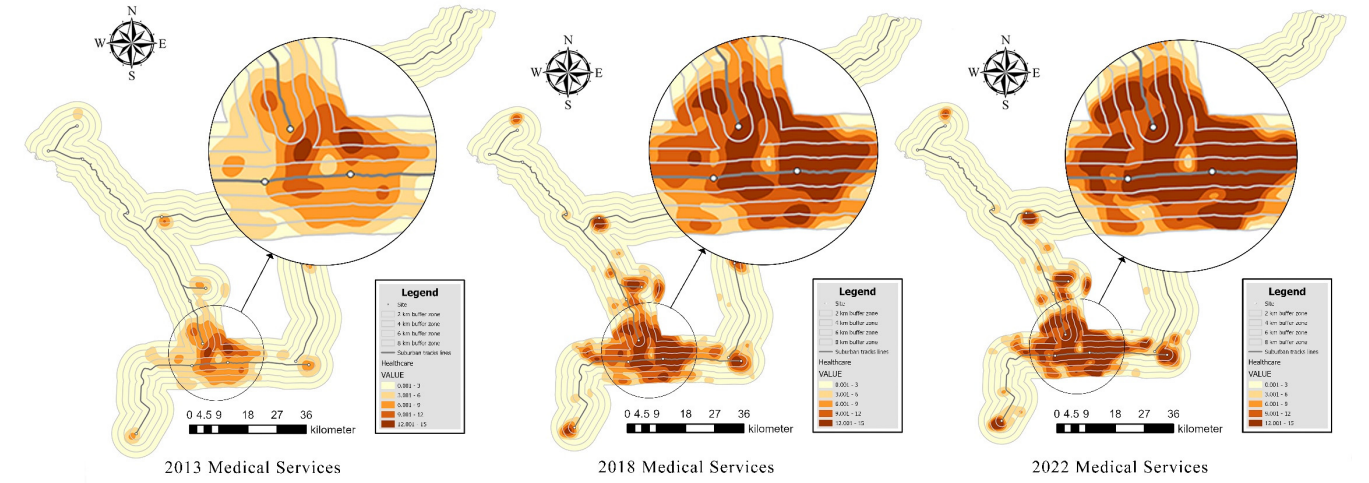

(**a**)

(**b**)

Figure 13. Detailed diagram of the medical services function. (**a**) Density analysis of the distribution of POIs for medical services in the 0–8 km buffer zone of the Beijing Suburban Railway at different time periods; (**b**) Sample collection points for COVID-19.

5.3. Limitations and Future Research Directions

By analyzing the spatio-temporal characteristics of urban expansion along Beijing's suburban railways, this paper reinforces the perception of urban expansion in megacities and provides valuable insight into suburban rail transit and urban expansion in China, but it is not without its limitations. Firstly, the findings of this paper are not necessarily applicable to urban expansion characteristics along suburban railroads in all megacities at home and abroad. In the future, it is essential to undertake a comprehensive investigation encompassing all suburban railways within a megacity cluster, rather than focusing solely on the suburban rail systems of an individual city or a select few. The expansion of megacities at different stages of development shows obvious differences, and studying urban expansion along all suburban railways in megacities helps to explore the mechanisms of urban expansion influenced by their rail transit systems.

Secondly, due to the high frequency of land cover changes in Beijing, using four-year intervals may not capture more detailed temporal changes in urban expansion along suburban railways. Shortening the inter-annual interval and lengthening the time span of the analysis allows for a more detailed understanding of the temporal characteristics of how suburban rail and even public rail transit impacts urbanization, which can help to understand the evolution of urban expansion within the public transit buffer.

Thirdly, the multi-source data used in this paper were not perfect due to data availability, such as point-of-interest data in the buffer zone. POIs are all abstract points without area, volume, and shape, which do not reflect the scale and intensity of the industry, and the location of the point deviates to some extent from the real location of the industry [86]. Therefore, the degree of urban expansion in the buffer zone can be analyzed in conjunction

with the calculation of the urban sprawl index (USI) and, at the same time, field research should be undertaken to further coordinate and correct the POI data obtained from e-maps.

Finally, cities are complex systems characterized by multiple heterogeneities, and multidimensional indicators of urban expansion can provide a more comprehensive picture of the spatio-temporal evolutionary characteristics of urban expansion or urbanization. Therefore, this paper only studied the spatial characteristics of urban expansion along suburban railways and did not expand socio-economic and other factors, which is not conducive to an accurate and comprehensive grasp of the interaction between urban expansion and suburban railways and their evolutionary patterns. In the future, we can try to apply more dimensional evaluation indicators such as demographic and economic indicators of suburban railways in different regional scopes. Combining urban spatial indicators with these two types of indicators to construct a more complete evaluation system will provide more valuable insight for understanding the evolution of urban expansion along suburban railways.

6. Conclusions

Understanding the growth patterns of megacities contributes to a better understanding of the global urbanization process in order to manage its growth [87], which is an important step towards global urban sustainability. However, the formation of megacities is not only reflected in planning but also in sharing various types of infrastructure, especially transport facilities. In recent years, with the national policy to support the construction of suburban railways and the introduction of a series of standards for suburban railways, the Beijing suburban railway is a realistic need for the megacity of Beijing to reach a certain stage of development. Therefore, taking the megacity of Beijing as an example, using remote sensing image and point-of-interest data in 2008, 2013, 2018, and 2022, and applying the standard deviation ellipse, the GIS center of gravity model, kernel density analysis, and landscape shape indexes, this paper investigated the spatio-temporal characteristics of urban expansion changes in the buffer zone along the Beijing suburban railway. In analyzing the urban form and function and landscape indexes within the buffer zone along the suburban railway, the specific conclusions are set out below:

First, the rate of urban expansion within the 8 km buffer zone of the Beijing suburban railway was highest during the planning period (2008–2013) and lowest during the construction period (2013–2018). In addition, the suburban railway had the greatest impact on built-up areas along 2–4 km of the route, with impacts diminishing after 4 km.

Second, within the 8 km buffer zone of the Beijing suburban railway, the expansion direction of the built-up area of the city shifted northward in the direction of latitude and eastward in the direction of longitude since 2008–2022, and the latitudinal direction shifted more obviously. The fastest rate of offset was during 2008–2013, at a rate of 322 m per year.

Third, in terms of landscape indicators, the degree of fragmentation in the built-up area was highest in the 2–4 km buffer zone and decreased to its lowest in the 6–8 km buffer zone. The PD, ED, LPI, and AI indicators showed a decreasing trend from year to year, while the LSI and COHESION indicators gradually increased, but the COHESION index decreased with the expansion of the buffer zone.

Finally, in terms of urban functions, the number of medical services surged in 2018–2022 while the numbers of the other three urban functions declined. The three urban functions other than scenic spots were mainly located in the main urban area, with very few clusters located near stations. The functions were distributed at the highest density in the 2–4 km buffer zone and at the lowest density in the 6–8 km buffer zone.

In summary, these findings contribute to a better understanding of the way urban expansion evolves within the gradient buffer zone along suburban railways and to the formulation of sustainable development planning strategies and urban transport policies for relevant authorities to achieve healthy, green, and sustainable development of urban transport.

Author Contributions: Conceptualization, writing—review and editing, validation, project administration, H.T. and J.Z.; supervision, H.T.; resources, J.Z.; visualization, software, formal analysis, investigation, X.Y. and T.L.; methodology, data curation, writing—original draft preparation, X.Y. All authors have read and agreed to the published version of the manuscript.

Funding: This research was funded by 2021 Research Project on Social Science Innovation and Development in Anhui Province (Grant No. 2021CX137), 2022 Key Projects of the Research Program of Anhui Universities (Philosophy and Social Sciences) (Grant No. 2022AH050863), 2022 General Project of Excellent Young Talents Support Program of Anhui Province Universities (Grant No. gxyq2022002), the Talent Research Grant of Anhui Agricultural University (Grant No. yj2022-52), and Anhui University Research Project (Grant No. 2023AH050968).

Data Availability Statement: The data for this study are available upon request from the authors.

Conflicts of Interest: The authors declare no conflict of interest.

References

1. Li, H.; Peng, J.; Liu, W.R.; Huang, Z.W. Stationary Charging Station Design for Sustainable Urban Rail Systems: A Case Study at Zhuzhou Electric Locomotive Co. *Sustainability* **2015**, *7*, 465–481. [CrossRef]
2. Sekar, S.P.; Gangopadhyay, D. Impact of Rail Transit on Land Use and Development: Case Study of Suburban Rail in Chennai. *J. Urban Plan. Dev.* **2017**, *6*, 143. [CrossRef]
3. Dong, H. If You Build Rail Transit in Suburbs, Will Development Come? *J. Am. Plan. Assoc.* **2016**, *82*, 316–326. [CrossRef]
4. Li, S.; Liu, X.; Li, Z.; Wu, Z.; Yan, Z.; Chen, Y.; Gao, F. Spatio-temporal Dynamics of Urban Expansion along the Guangzhou-Foshan Inter-City Railway Transit Corridor, China. Transit Corridor, China. *Sustainability* **2018**, *10*, 593. [CrossRef]
5. Ministry of Housing and Urban-Rural Development of the People's Republic of China. *Statistical Yearbook of Urban and Rural Construction 2021*; Ministry of Housing and Urban-Rural Development of the People's Republic of China: Beijing, China, 2021.
6. Bhatta, B.; Saraswati, S.; Bandyopadhyay, D. Urban sprawl measurement from remote sensing data. *Appl. Geogr.* **2010**, *30*, 731–740. [CrossRef]
7. Dai, J.; Gao, X.; Du, S. Expansion of Urban Space and land cover Control in the Process of Urbanization: An Overview. *Chin. J. Popul. Resour. Environ.* **2010**, *8*, 73–82.
8. Buyantuyev, A.; Wu, J.; Gries, C. Multiscale Analysis of the Urbanization Pattern of the Phoenix Metropolitan Landscape of USA: Time, Space and Thematic Resolution. *Landsc. Urban Plan.* **2015**, *94*, 206–217. [CrossRef]
9. Hecht, R.; Behnisch, M.; Herold, H. Innovative Approaches, Tools and Visualization Techniques for Analysing land cover Structures and Dynamics of Cities and Regions (Editorial). *J. Geovisualization Spat. Anal.* **2020**, *4*, 19. [CrossRef]
10. Rusk, D. *Cities without Suburbs*; Woodrow Wilson Center Press: Washington, DC, USA, 1993.
11. Taubenbock, M.H.; Wegmann, A.; Roth, H.; Mehl, S. Dech Urbanization in India—Spatiotemporal analysis using remote sensing data. *Comput. Environ. Urban Syst.* **2009**, *33*, 179–188. [CrossRef]
12. Kantakumar, L.N.; Kumar, S.; Schneider, K. Spatiotemporal Urban Expansion in Pune metropolis, India Using Remote Sensing. *Habitat Int.* **2016**, *51*, 11–22. [CrossRef]
13. Frohn, H.; Frohn, R.C.; Hao, Y. Landscape metric performance in analyzing two decades of deforestation in the Amazon Basin of Rondonia, Brazil. *Remote Sens. Environ.* **2006**, *100*, 237–251. [CrossRef]
14. Wang, H.; Zhang, B.; Liu, Y.; Liu, Y.; Xu, S.; Zhao, Y.; Chen, Y.; Hong, S. Urban expansion patterns and their driving forces based on the center of gravity-GTWR model: A case study of the Beijing-Tianjin-Hebei urban agglomeration. *J. Geogr. Sci.* **2020**, *30*, 297–318. [CrossRef]
15. Huang, D.; Chu, E.; Liu, T. Spatial Determinants of Land Conversion for Various Urban Use: A Case Study of Beijing. *ISPRS Int. J. Geo-Inf.* **2020**, *9*, 708. [CrossRef]
16. Mozaffaree Pour, N.; Oja, T. Prediction Power of Logistic Regression (LR) and Multi-Layer Perceptron (MLP) Models in Exploring Driving Forces of Urban Expansion to Be Sustainable in Estonia. *Sustainability* **2022**, *14*, 160. [CrossRef]
17. Chen, X.; Zhang, K. Urban Area Characterization and Structure Analysis: A Combined Data-Driven Approach by Remote Sensing Information and Spatial-Temporal Wireless Data. *Remote Sens.* **2023**, *15*, 1041. [CrossRef]
18. Garcia-Ayllon, S. Rapid development as a factor of imbalance in urban growth of cities in Latin America: A perspective based on territorial indicators. *Habitat Int.* **2016**, *58*, 127–142. [CrossRef]
19. Xu, Q.; Zheng, X.; Zhang, C. Quantitative Analysis of the Determinants Influencing Urban Expansion: A Case Study in Beijing, China. *Sustainability* **2018**, *10*, 1630. [CrossRef]
20. Huang, Q.; Huang, J.; Yang, X.; Ren, L.; Tang, C.; Zhao, L. Evaluating the scale effect of soil erosion using landscape shape metrics and information entropy: A case study in the Danjiangkou reservoir area, China. *Sustainability* **2017**, *9*, 1243. [CrossRef]
21. Fu, Y. *Study on the Development of Edge Areas of Megacities under the Influence of Rail Transit Suburban Lines*; Tianjin University: Tianjin, China, 2020.

22. The Relevant Responsible Comrade of the State Railway Administration Answered Reporters' Questions on the Release of the Design Code for Municipal (Suburban) Railway. Official Website of State Railway Administration of China, 28 December 2020. Available online: https://www.nra.gov.cn/ (accessed on 11 December 2022).
23. National Bureau of Statistics of China. *Statistical Tables and Charts on Economic and Social Development, National Bureau of Statistics of China: Basic Information on the Population of Very Large and Mega Cities in the Seventh National Census*; National Bureau of Statistics of China: Beijing, China, 2020.
24. Ji, C. *A Study on Countermeasures for Conflicts of Environmental Neighboring Facilities in Mega Cities*; East China University of Politics and Law: Shanghai, China, 2020.
25. Yu, S.; Zhang, Z.; Liu, F.; Wang, X.; Hu, S. Urban expansion in the megacity since 1970s: A case study in Mumbai. *Geocarto Int.* **2019**, *36*, 603–621. [CrossRef]
26. Cai, E.; Bi, Q.; Lu, J.; Hou, H. The Spatiotemporal Characteristics and Rationality of Emerging Megacity Urban Expansion: A Case Study of Zhengzhou in Central China. *Environ. Inform. Remote Sens.* **2022**, *10*, 860814. [CrossRef]
27. Chen, C.; Richard, L.; Fang, C. From coordinated to integrated urban and rural development in China's megacity regions. *J. Urban Aff.* **2018**, *41*, 150–169. [CrossRef]
28. Aritenang, A.F. The contribution of foreign investment and industrial concentration to firm competitiveness in Jakarta Megacity. *Cities* **2021**, *113*, 103152. [CrossRef]
29. Hu, X.; Yang, H.; Yang, J.; Zhang, Z. Spatial Correlation Network of Format in the Central Districts of a Megacity: The Case of Shanghai. *Sustainability* **2019**, *11*, 5191. [CrossRef]
30. Wang, K.-L.; Xu, R.-Y.; Cheng, Y.-H. Understanding the overall difference, distribution dynamics and convergence trends of green innovation efficiency in China's eight urban agglomerations. *Ecol. Indic.* **2023**, *148*, 110101. [CrossRef]
31. Zha, Q.; Liu, Z.; Song, Z. A study on dynamic evolution, regional differences and convergence of high-quality economic development in urban agglomerations: A case study of three major urban agglomerations in the Yangtze river economic belt. *Front. Environ. Sci.* **2022**, *10*, 1012304. [CrossRef]
32. Zhao, J. Construction of high-speed passenger railways will cause serious damage to China's economy. *Explor. Railw. Econ. Issues* **2009**, 157–166.
33. Zhang, Y. *Evaluation and Optimization Method of Part-Time Suburban Railway under the Perspective of Commuting Circle*; Beijing Jiaotong University: Beijing, China, 2022.
34. Aoki, Y.; Osaragi, T.; Ishizaka, K. An interpolating model for land-price data with transportation costs and urban activities Environment and Planning B. *Plan. Des.* **1994**, *21*, 53–65.
35. Batista, R.M.G. O aproveitamento de antigas infraestruturas ferroviárias em meio urbano: As ecopistas como exemplo. Master's Thesis, University of Porto, Porto, Portugal, 2015.
36. Sultana, S.; Weber, J. The Nature of Urban Growth and the Commuting Transition: Endless Sprawl or a Growth Wave? *Urban Stud.* **2014**, *51*, 544–576. [CrossRef]
37. Chiara, M.; Travisi Roberto, C.; Peter, N. Impacts of urban sprawl and commuting: A modelling study for Italy. *J. Transp. Geogr.* **2010**, *18*, 382–392.
38. Dubé, J.; Thériault, M.; Rosiers, F.D. Commuter rail accessibility and house values: The case of the Montreal South Shore, Canada, 1992–2009. *Transp. Res. Part A* **2013**, *54*, 49–66. [CrossRef]
39. Xia, X.; Li, H.; Kuang, X.; Strauss, J. Spatial-Temporal Features of Coordination Relationship between Regional Spatial-Temporal Features of Coordination Relationship between Regional Urbanization and Rail Transit-A Case Study of Beijing. *J. Environ. Res. Public Health* **2022**, *19*, 212. [CrossRef] [PubMed]
40. Rode, P.; Floater, G.; Thomopoulos, N.; Docherty, J.; Schwinger, P.; Mahendra, A.; Fang, W. Accessibility in Cities: Transport and Urban Form. In *Disrupting Mobility: Impacts of Sharing Economy and Innovative Transportation on Cities*; Meyer, G., Shaheen, S., Eds.; Lecture Notes in Mobility; Springer International Publishing: Cham, Switzerland, 2017; pp. 239–273.
41. Chiang, C.M. History, characteristics and experience of rail transit development in Tokyo metropolitan area. *Compr. Transp.* **2021**, *43*, 119–125.
42. Beijing Municipal Bureau of Statistics. *Beijing Statistical Yearbook 2020*; Beijing Municipal Bureau of Statistics: Beijing, China, 2020.
43. Reply of the State Council of the Central Committee of the Communist Party of China to the Approval of the Beijing Urban Master Plan (2016–2035). Official Website of the Central People's Government of the People's Republic of China. 27 September 2017. Available online: http://www.beijing.gov.cn/ (accessed on 11 December 2022).
44. Wang, D. Reflections on the Construction of Beijing Suburban Railway. *J. Beijing City Coll.* **2021**, *166*, 6–10+26.
45. Yue, L. *A Study on Job-Life Relationship and Commuting Performance in Megacities*; East China Normal University: Shanghai, China, 2023; p. 22.
46. Chai, Y.; Zhang, X.; Sun, D. A study on urban living area planning based on spatio-temporal behaviors—Taking Beijing as an example. *J. Urban Plan.* **2015**, *3*, 61–69.
47. Zhang, Q. Spatial coupling of station influence domain and community living circle—Taking the example of Chongqing, a mountainous urban environment as an example. *J. Chongqing Univ. Technol. (Nat. Sci.)* **2020**, *34*, 202–210.
48. Xiong, W.; Xu, Y. Study on Urban Habitat Environment Based on the Perspective of Public Facilities—Taking Nanjing as an Example. *Mod. Urban Res.* **2010**, *25*, 35–42.

49. Zhang, Y. Traffic Factors and Optimization Strategies of 15-Minute Living Circle Travel Influence—An Empirical Analysis of Six Typical 15-Minute Living Circles in Wuhan City. China Society of Urban Planning, Chongqing Municipal People's Government. Vibrant Urban and Rural Areas and Beautiful Habitat. In Proceedings of the 2019 China Urban Planning Annual Conference (20 Housing and Community Planning), Chongqing, China, 19–21 October 2019; China Architecture Industry Press: Beijing, China, 2019; pp. 803–816.
50. Dai, F.; Diao, M.; Sing, T. A two-dimensional propensity score matching approach to estimating the treatment effect of urban rail transit lines on vehicle travel. *Transportation* **2022**. [CrossRef]
51. Liu, Q. Influential elements of TOD area planning circle structure division. *Int. Urban Plan.* **2017**, *32*, 72–79. [CrossRef]
52. Zhan, Z.; Li, L.; Wu, H. Experience and inspiration of pedestrian space planning in TOD areas of Korean rail stations. *Planner* **2022**, *38*, 38–146.
53. Cao, X. Review and outlook of research on community built environment and traffic behavior: A lesson from the United States. *Int. Urban Plan.* **2015**, *30*, 46–52.
54. Ta, N.; Zeng, Y.; Zhu, Q.; Wu, J. Analysis of the relationship between built environment and urban vitality in central Shanghai based on big data. *Geoscience* **2020**, *40*, 60–68.
55. Ren, J. *Research on the Impact of Job and Residence Separation on the Travel of Shared Bicycle Users*; Beijing Jiaotong University: Beijing, China, 2022.
56. Cao, Y.; Zhang, X.; Li, F.; Shu, K. Analysis of the coupling relationship between land cover and bike sharing around rail transit stations—Taking Xi'an as an example. *China Transp. Rev.* **2022**, *44*, 163–170.
57. Cao, Y. *A Study on the Accessibility Analysis of Rail Transit Stations and the Layout of Interchange Facilities Considering the Connection of Shared Bicycles*; Southeast University: Nanjing, China, 2020.
58. Zhou, Q.; Chen, D.; Chen, Q. A study on land cover center of gravity migration in the mountainous metropolitan area of Chongqing from 1985 to 2010. *Res. Soil Water Conserv.* **2013**, *20*, 189–193.
59. Yang, Y.; Liu, Y.; Li, Y.; Du, G. Quantifying spatio-temporal patterns of urban expansion in Beijing during 1985–2013 with rural-urban development transformation. *Land Use Policy* **2018**, *74*, 220–230. [CrossRef]
60. Chen, Y.M.; Li, X.; Liu, X.P.; Ai, B. Modeling urban land-use dynamics in a fast developing city using the modified logistic cellular automaton with a patch-based simulation strategy. *Int. J. Geogr. Inf. Sci.* **2014**, *28*, 234–255. [CrossRef]
61. Tong, L. *A Study on Generalized Urban Expansion Metric and Its Application*; China University of Geosciences: Wuhan, China, 2018.
62. Xu, X.L.; Min, X.B. Quantifying spatiotemporal patterns of urban expansion in China using remote sensing data. *Cities* **2013**, *25*, 104–113. [CrossRef]
63. Tu, Y.; Chen, B.; Yu, L. How does urban expansion interact with cropland loss? A comparison of 14 Chinese cities from 1980 to 2015. *Landsc. Ecol.* **2021**, *36*, 243–263. [CrossRef]
64. Liu, L.; Xiang, Y. Spatio-temporal analysis of commercial space pattern and industry distribution in urban Nanjing based on POI data. *Nat. Resour. Informatiz.* **2023**, *2*, 71–77.
65. Zhou, N. Research on urban spatial structure based on the dual constraints of geographic environment and POI big data. *J. King Saud Univ. Sci.* **2022**, *34*, 101887. [CrossRef]
66. Dietzel, C.; Herold, M.; Hemphill, J.J.; Clark, K.C. Spatio-temporal dynamics in California's Central Valley: Empirical links to urban theory. *Int. J. Geogr. Inf. Sci.* **2005**, *19*, 175–195. [CrossRef]
67. Araya, Y.H.; Cabral, P. Analysis and modeling of urban land cover change in Setúbal and Sesimbra, Portugal. *Remote Sens.* **2010**, *2*, 1549–1563. [CrossRef]
68. Nassar, A.K.; Blackburn, G.A.; Whyatt, D. Developing the desert: The pace and process of urban growth in Dubai. *Comput. Environ. Urban Syst.* **2014**, *45*, 50–62. [CrossRef]
69. Taubenböck, H.; Wiesner, M.; Felbier, A.; Marconcini, M.; Esch, T.; Dech, S. New dimensions of urban landscapes: The spatio-temporal evolution from a poly nuclei area to a mega-region based on remote sensing data. *Appl. Geogr.* **2014**, *47*, 137–153. [CrossRef]
70. Luck, M.; Wu, J. A gradient analysis of urban landscape shape: A case study from the Phoenix metropolitan region, Arizona, USA. *Landsc. Ecol.* **2002**, *17*, 327–339. [CrossRef]
71. Zhu, M.; Xu, J.G.; Jiang, N.; Li, J.L.; Fan, Y. Impacts of road corridors on urban landscape shape: A gradient analysis with changing grain size in Shanghai, China. *Landsc. Ecol.* **2006**, *21*, 723–734. [CrossRef]
72. Tan, K.C.; Lim, H.S.; MatJafri, M.Z.; Abdullah, K. Landsat Data to Evaluate Urban Expansion and Determine land cover/land Cover Changes in Penang Island, Malaysia. *Environ. Earth Sci.* **2010**, *60*, 1509–1521. [CrossRef]
73. Wang, X.; Shi, R.; Zhou, Y. Dynamics of urban sprawl and sustainable development in China. *Socio-Econ. Plan. Sci.* **2020**, *70*, 100736. [CrossRef]
74. Shi, Y.; Zhou, L.; Guo, X.; Li, J. The Multidimensional Measurement Method of Urban Sprawl and Its Empirical Analysis in Shanghai Metropolitan Area. *Sustainability* **2023**, *15*, 1020. [CrossRef]
75. Zhao, P. Sustainable urban expansion and transportation in a growing megacity: Consequences of urban sprawl for mobility on the urban fringe of Beijing. *Habitat Int.* **2010**, *34*, 236–243. [CrossRef]
76. Liu, Y. *Utilization of Existing Railways in the Development of Rail Transportation in Large Cities*; Beijing Jiaotong University: Beijing, China, 2015.

77. Pradhan, B. *Spatial Modeling and Assessment of Urban Form: Analysis of Urban Growth: From Sprawl to Compact Using Geospatial Data*; Springer International Publishing: New York, NY, USA, 2017.
78. Frenkel, A.; Ashkenazi, M. Measuring Urban Sprawl: How Can We Deal with It? *Environ. Plan. B Plan. Des.* **2008**, *35*, 56–79. [CrossRef]
79. Vwlvavn, T.P.; Meyer, C.G. The COVID-19 epidemic. *Trop. Med. Int. Health* **2020**, *25*, 278–280.
80. Zheng, R. Spatial transmission of COVID-19 via public and private transportation in China. *Travel Med. Infect. Dis.* **2020**, *34*, 101626. [CrossRef] [PubMed]
81. Deng, S. *A Study on Public Service Provision of Compulsory Education in Y County under the Background of "Double Reduction" Policy*; Jilin University of Finance and Economics: Changchun, China, 2022.
82. Liang, S. *A study on the Enhancement Strategy of Rural Road Spatial Planning in Xi'an under Ecological Orientation*; Chang'an University: Xi'an, China, 2019.
83. Tang, W.; Cui, Q.; Zhang, F.; Yan, H. Evaluation of the land value-added benefit brought by urban rail transit: The case in Changsha, China. *J. Transp. Land Cover* **2021**, *14*, 563–582. [CrossRef]
84. Liu, J.; Feng, A.; Wang, J.; He, P.; Deng, J. Development strategy of suburban rail transit in Beijing. *Urban Transp. China* **2014**, *12*, 28–36.
85. Wang, S.Y.; Liu, Y.; Chen, Z.D. Representing multiple urban places' footprints from Dianping.com data. *Acta Geod. Cartogr. Sin.* **2018**, *47*, 1105–1113.
86. Vasenev, I.; Dovletyarova, E.; Chen, Z.; Valentini, R. Megacities 2050: Environmental consequences of urbanization. In Proceedings of the Conference on Landscape Architecture to Support City Sustainable Development, Moscow, Russia, 12–14 September 2016; RUDN-People's Friendship University of Russia: Moscow, Russia; pp. 12–24.
87. Kraas, F. Megacities and global change: Key priorities. *Geogr. J.* **2007**, *173*, 79–82. [CrossRef]